IOPscience iopscience.iop.org

Home Search Collections Journals About Contact us My IOPscience

Nanostructured target fabrication with metal and semiconductor nanoparticles

This content has been downloaded from IOPscience. Please scroll down to see the full text.

2015 Mater. Res. Express 2 105005

(http://iopscience.iop.org/2053-1591/2/10/105005)

View the table of contents for this issue, or go to the journal homepage for more

Download details:

IP Address: 192.77.52.4
This content was downloaded on 06/10/2015 at 20:19

Please note that terms and conditions apply.

Materials Research Express

PAPER

Nanostructured target fabrication with metal and semiconductor nanoparticles

RECEIVED
20 April 2015

REVISED
2 July 2015

ACCEPTED FOR PUBLICATION
7 July 2015

PUBLISHED
5 October 2015

M Barberio[1] and P Antici[2]

[1] DiBEST department, University of Calabria and INFN, Italy; ELI-ALPS, Szeged, Hungary
[2] INRS-EMT, Varennes, Canada; ELI-ALPS, Szeged, Hungary; University of Rome, dip. SBAI and INFN, Italy

E-mail: marianna.barberio@fis.unical.it **and** antici@emt.inrs.ca

Keywords: laser-driven acceleration, nanostructured target, semiconductive target

Abstract

The development of ultra-intense high-energy (≫1 J) short (<1 ps) laser pulses in the last decade has enabled the acceleration of high-energy short-pulse proton beams. A key parameter for enhancing the acceleration regime is the laser-to-target absorption, which heavily depends on the target structure and material. In this work, we present the realization of a nanostructured target with a sub-laser wavelength nano-layer in the front surface as a possible candidate for improving the absorption. The nanostructured film was realized by a simpler and cheaper method than using conventional lithographic techniques: A colloidal solution of metallic or semiconductor nanoparticles (NPs) was produced by laser ablation and, after a heating and sonication process, was spray-dried on the front surface of an aluminum target. The obtained nanostructured film with a thickness of 1 μm appears, at morphological and chemical analysis, uniformly nanostructured and distributed on the target surface without the presence of oxides or external contaminants. Finally, the size of the NPs can be tuned from tens to hundreds of nanometers simply by varying the growth parameters (i.e., irradiation time, fluence, and laser beam energy).

1. Introduction

Efficient absorption of pulsed laser energy by the target is a key parameter in the laser-driven production of energetic protons and electrons for different applications. Within the standard proton acceleration process, also often called target normal sheath acceleration (TNSA) [1], a critical question is the generation, at the front side of the target, of hot electrons with the highest values of density [2, 3], energy, and collimation, while another important factor for best acceleration is its transport through the bulk of the target [4]. Recently, several groups [5–7] demonstrated, experimentally and using two-dimensional particle-in-cell simulations, that nanostructured targets can enhance laser absorption [8]. In particular, a target with a sub-wavelength nano-layered front surface can reduce the laser reflection at the front side and increase the energy absorption of an intense, short laser pulse. Moreover, the efficiency of particle production and laser/particle energy transfer can be increased with a properly shaped nano-pattern realized on the target surface.

In this context, many research groups work on the realization of nano- and microstructured targets and on the investigation (with both experimental and theoretical approaches) of better targets. Strong efforts have been made in the realization of a polymeric, metallic, or semiconductor target with a nanostructured surface realized by chemical reactions on surfaces, insertion of carbon-based nanomaterials (specially carbon nanotubes, nanofibers, and fullerenes), or by the use of x-ray lithography [9–11]. Many of these methods require very long and expensive processes without allowing a good control of the shape or dimension of the realized nano-pattern.

In this work, we propose a simple method to realize targets with a nanostructured layer constituted by metallic (Al) or semiconductor (ZnSe) nanoparticles (NPs) [12, 13]. We realize the nanostructured layer on aluminum targets, because the wetting properties between aluminum and metal or semiconductor NPs can ensure the realization of a uniform nanostructured film on the surface without local aggregation of NPs [14]. The film was realized with the spray-dry technique applying on the target surface a colloidal solution containing

© 2015 IOP Publishing Ltd

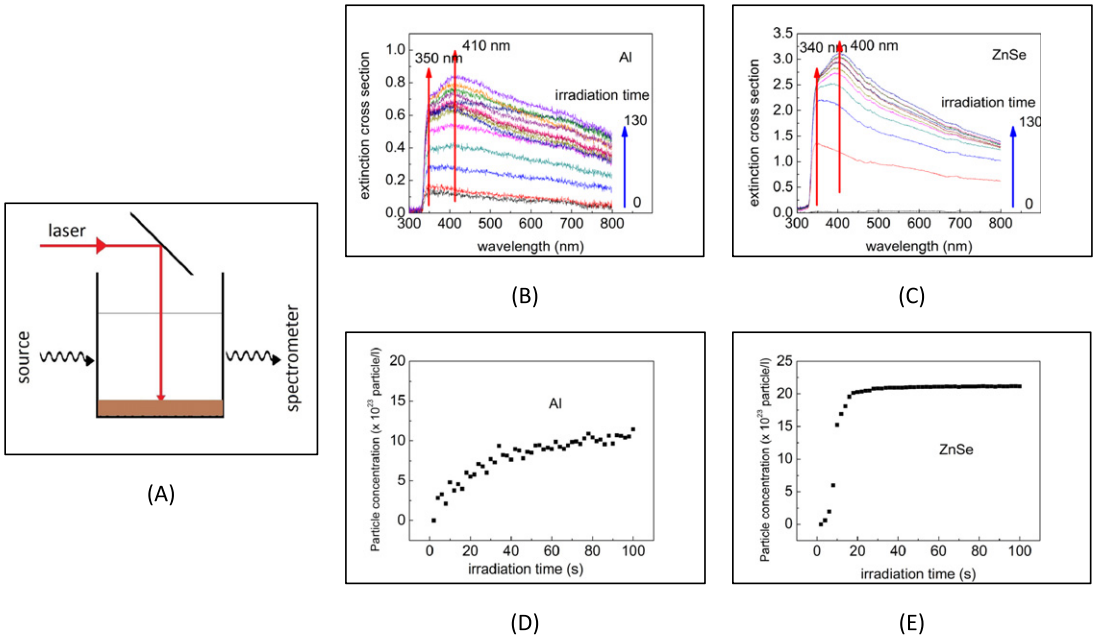

Figure 1. Sketch of LASiS experimental setup (A); cross sections of Al (B) and ZnSe (C) colloidal solutions taken at regular intervals of 10 s from irradiation; time evolution of the particle concentration in solution for Al (D) and ZnSe (E) NPs.

metal or semiconductor NPs grown by laser ablation in solution (LASiS). All of the produced targets were characterized by conventional microscopies and spectroscopies to better understand the morphological and chemical properties of the nanostructured film.

2. Materials and methods

2.1. Materials

ZnSe and Al NPs were produced by the LASiS process. 250 mg of ZnSe grains or a sheet of Al (manufactured by Goodfellow with a purity >99.9%) were deposed in a cuvette containing 10 ml of acetone and ablated with the first harmonic (1064 nm) of a pulsed YAG Laser (7100 series of Quanta System). The laser has a fluence of 500 mJ cm^{-2}, pulse duration of 7 ns, a repetition rate of 20 pulses/s, and a spot size on the target of about 1 cm^2. The target was irradiated in aerobic conditions for 120 s, and during the irradiation, the absorbance spectra and the coloration of the colloidal solution were checked at regular time intervals of 2 s (a sketch of the experimental setup is illustrated in figure 1(a)) to estimate shape, dimensions, and concentration of the produced particles (following the Mie exact theory of extinction [15–17]). When the irradiation stopped, a droplet of 50 μl of the colloidal solution was deposed on a SiO_2 plate (size of about 2 cm^2) to take morphological and chemical analyses, as described below.

After the NP growth, 50 ml of colloidal solution were heated on a hot plate at 80 °C for 30 min until the evaporation of about 80% of the solvent; after this, the solution was cooled down to room temperature and sonicated for 1 h to reduce the particle aggregation caused by the increase of the particle concentration in the solution. During the heating and sonication phases the colloidal solution was stable, without signs of particle aggregation or changes in optical absorption, as demonstrated in [18]. The obtained colloidal solution was spray-dried on an Al target (Goodfellow, nominal purity greater than 99.9%) and heated on a hot plate at 80 °C until the complete evaporation of the solvent. The low value of the evaporation temperature has been chosen for preventing the NPs' oxidation. Both targets were then analyzed by scanning electron microscopy and electron dispersion x-ray (SEM-EDX) to obtain morphological and chemical information.

2.2. Methods

Morphological analysis of both NPs and targets were conducted by SEM and atomic force microscopy (AFM).

AFM images were obtained by the ICON AFM microscope from Bruker, working in tapping mode. Each image was taken with a resolution of 512 × 512 pixels and a frequency of about 1 Hz. The shapes and dimensions of the NPs were analyzed, conducting a statistical analysis on many NPs collected in several AFM images. For each sample, we scanned several areas in a window of 500 nm × 500 nm, 1 μm × 1 μm, and 5 μm × 5 μm. The

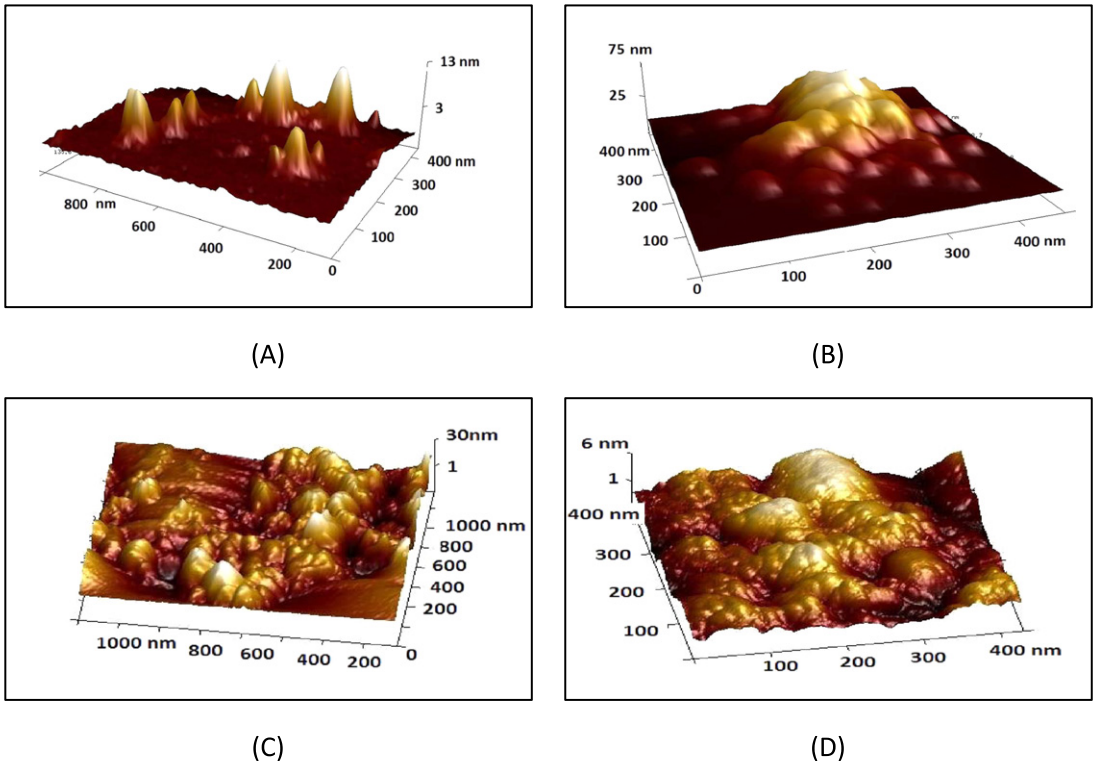

Figure 2. AFM 3D images showing the nanoparticles collected after an irradiation time of 35 s and 120 s. (A) and (B): Al NPs; (C) and (D): ZnSe NPs.

images were then elaborated by the Nanoscope software (version 1.40 from Bruker) to obtain three-dimensional (3D) structures and to measure the dimensions.

The radius of each NP was evaluated assuming a spherical shape. Due to the high wetting properties of Al and ZnSe on the silicon dioxide surface, the NP rests on the SiO_2 surface, forming a spherical cap-like structure with a low contact angle. We can evaluate the radius r_i of each NP, assuming that the volume of the spherical particle is conserved in the deposition process.

SEM images were taken under a STEREOSCAN SEM microscope, working with an energy of 20 keV.

Measurements of optical absorption during the laser irradiation were obtained irradiating the solution with a white lamp (Energetiq LDLS, Laser Driven Light Source), and the transmitted spectra were taken by a Triax 320 (HORIBA Jobyn Yvon) spectrometer working in the 300–800 nm range. The extinction cross section and optical absorption were evaluated using the standard equations:

$$\in(\lambda) = -Log\frac{I_t(\lambda)}{I_0(\lambda)} \tag{1}$$

$$a(\lambda) = 1 - \frac{I_t(\lambda)}{I_0(\lambda)} \tag{2}$$

where I_t and I_0 are, respectively, the transmitted and source intensity at each wavelength. The particle concentration at irradiation time was evaluated by the Lambert and Beer's Law:

$$\varepsilon\left(\lambda_p\right) = c^{\star}\alpha^{\star}l \tag{3}$$

where $\varepsilon\ (\lambda_p)$ is the extinction cross section at the wavelength of the plasmonic oscillation (λ_p), c is the particle concentration, α the molar extinction cross section at λ_p (tabulated for each wavelength in [19]), and l the optical path length in our experimental setup (1 cm). We evaluated the particle concentration at the wavelength corresponding to the plasmonic peak in the extinction cross section, and additionally analyzed the behavior of primary particles produced by laser irradiation.

Chemical information on all samples was obtained from EDX spectroscopy under SEM conditions, realized simultaneously to the image acquisition, and from x-ray photoelectron spectroscopy (XPS). XPS measurements were conducted in an ultra-high vacuum chamber equipped for standard surface analysis with a base pressure in the range of low 10^{-9} torr. A non-monochromatic Mg-Kα x-ray ($h\nu = 1253.64$ eV) was used as excitation source. The XPS spectra were calibrated with the C1s peak of a pure carbon sample (binding energy 284.6 eV).

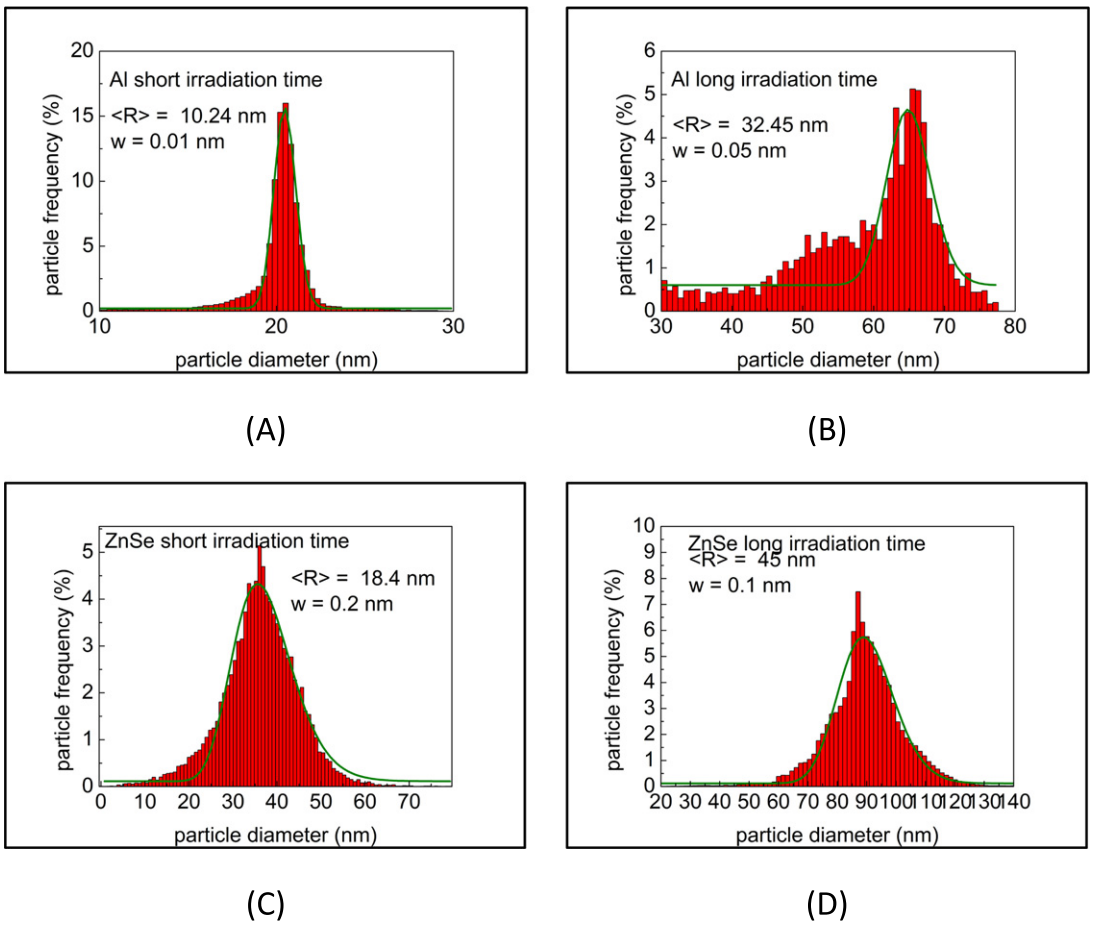

Figure 3. Histograms of particle radius distribution for nanoparticles collected after an irradiation time of 35 s and 120 s. (A) and (B): Al NPs; (C) and (D): ZnSe NPs.

3. Results and discussion

A collection of extinction cross sections taken during the laser irradiation is shown in figure 1(b) for Al NPs and 1(c) for ZnSe NPs. It is clear that the position of plasmonic oscillations changes for both materials during laser irradiation. In particular, we can observe that in the first 30 s of irradiation there is only a plasmonic peak in both cross-section spectra at about 350 nm for Al NPs and 340 nm for ZnSe NPs, corresponding in both cases to the formation of NPs with a radius of about 10 nm. For irradiation times greater than 30 s, for both NPs, we see a second plasmonic peak, at 410 nm for Al and 400 nm for ZnSe, corresponding to the formation of particles with a radius ranging from 40–50 nm. The analysis of the particle distribution (figures 1(d) and (e)), evaluated on the first plasmonic peak, indicates that the concentration of smaller particles linearly increases until 30 s and then reaches a saturation regime. The results of both, the cross section and the concentration evolution suggest that in the first 30 s only the primary particles produced by LASiS are present as colloidal in the solution. When the concentration of the primary particles reaches saturation, an aggregation process starts, causing the formation in the solution of a particle cluster with bigger dimensions (with a process similar to what was observed for silver NPs in our previous work [20]). Morphological analysis of a droplet of solution taken at two different irradiation times (35 s and 120 s) confirms these results. For a short irradiation time we observe in the AFM images (figures 2(a)–(d)) the formation, for both NP species, of NPs with different dimensions. The diameter distributions (figure 3) indicate that the NP diameters are distributed as a LogNorm function (typical for NP growth by laser ablation) with a small radius (10.24 and 18 nm for Al and ZnSe, respectively) for a short irradiation time. For a longer irradiation time they generate big aggregates (with radius of 45.2 nm and 32.45 nm for Al and ZnSe, respectively).

The AFM characterizations (not shown) of the solution spray-dried on an Al target confirm that the dimension of the NPs are those obtained at the end of the LASiS; aggregation is caused by the subsequent process of heating, concentration increase, sonication, and spray-dry.

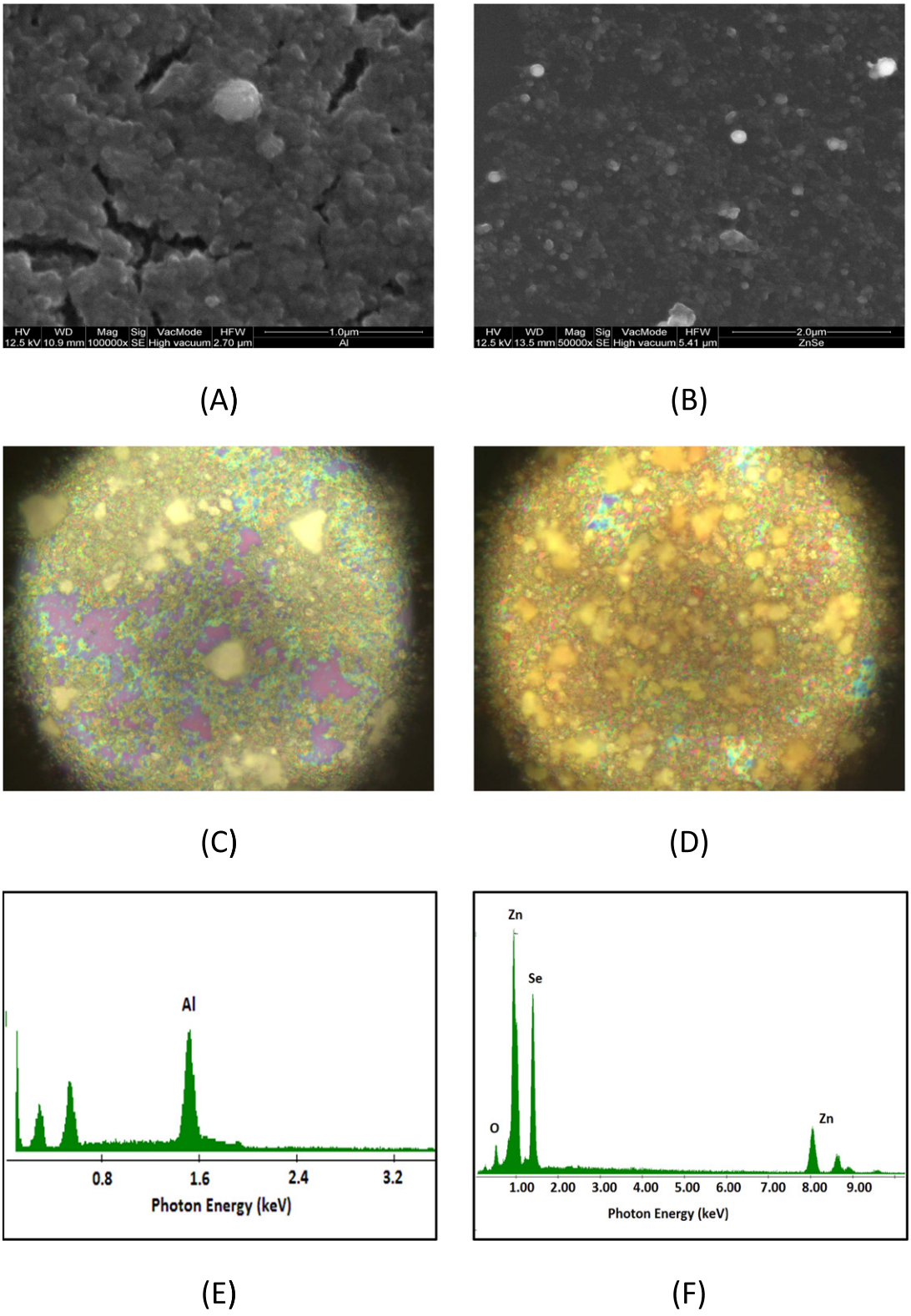

Figure 4. SEM ((A) and (B)) and optical ((C) and (D)) images of nanostructured films on target surface using Al and ZnSe NPs, respectively. EDX spectra for Al and ZnSe ((E) and (F)) nano-structured films.

SEM (figures 4(a) and (b)) and optical (figures 4(c) and (d)) images of NPs deposed on an Al target confirm the formation of a uniform layer with a thickness of about 1 micron of Al or ZnSe NPs completely covering the target surface. EDX analysis (figures 4(E) and (f)) indicates that the layer is composed only by the main element constituting the NPs, i.e., Al, Zn, or Se, without the presence of oxide or external impurities, which can change the target conductivity and the laser irradiation absorption. XPS measurements confirm the absence of oxides. In fact, the peak position of the main lines corresponding to the constitutive elements (Al 2p 72.85 eV, Zn 3p

88.76 eV, and Se 3d 54.1 eV) are close to those of pure elements [21], without any chemical shifts, indicating the presence of Al-O or Zn-O chemical bonds. XPS data indicate also a little presence of oxygen (about 2%) on the sample surfaces that can be attributed to adsorbed atmospheric oxygen.

4. Conclusions

In this work, we present the realization of a target with a sub-wavelength nano-layered front surface. The nanostructuration of the aluminum target front surface was realized with a method that is simpler and cheaper than conventional lithographic processes. NPs of metal (Al) and semiconductor (ZnSe) materials were produced by LASiS: The colloidal solution was first heated and then went through sonication phases for increasing the NP concentration; finally it was spray-dried on the target surface. The NP dimensions can be tuned simply by varying the irradiation time in LASiS; for short irradiation times the obtained nanostructures on the surface are particles with a radius of about 10 nm, while for longer irradiation times we can reach dimensions of hundreds of nanometers. The nanostructured film is uniform and coats the entire target surface without the presence of oxides or external impurities. This avoids the modification of the conductivity and the optical absorption of the target. The next step will be to simulate and then perform laser-driven proton acceleration experiments and measure the absorption in the different obtainable configurations.

Acknowledgments

The authors thanks Dr M. Davoli from UNICAL for SEM images. MB is supported by the Regional Operative Program (ROP) Calabria ESF 2007/2013—IV Axis Human Capital—Operative Objective M2, ARUE-Project CMN. This work is supported by CRISP (FP7 Contract No. 283745), FRQNT (nouveaux chercheurs, Grant No. 174726, 189974), the NSERC Discovery Grant (Grant No. 435416), Compute Canada (cng-261-01), and ELI-ALPS , Hungary (Project GOP-2012-1.1.1.-12/B-2012-0001).

References

[1] Wilks S C, Kruer W L, Tabak M and Langdon A B 1992 *Phys. Rev. Lett.* **69** 1383
[2] Antici P *et al* 2008 *Phys. Rev. Lett.* **101** 105004
[3] Nagai K *et al* 2006 *Appl. Phys. Lett.* **88** 094102
[4] Cao L, Gu Y, Zhao Z, Cao L, Huang W, Zhou W, He X T, Yu W and Yu M Y 2010 *Phys. Plasmas* **17** 043103
Brown C R D *et al* 2011 *Phys. Rev. Lett.* **106** 185003
[5] Andreev A, Kumar N, Platonov K and Pukhov A 2011 *Phys. Plasmas* **18** 103103
[6] Margarone D *et al* 2012 *Phys. Rev. Lett.* **109** 234801
[7] Yu J, Zhao Z, Jin X, Wu F, Yan Y, Zhou W, Cao L, Li B and Gu Y 2012 *Phys. Plasmas* **19** 053108
[8] Antici P, Gremillet L, Grismayer T, Mora P, Audebert P, Borghesi M, Cecchetti C A, Manic A and Fuchs J 2013 *Phys. Plasmas* **20** 123116
[9] Bagchi S, Prem Kiran P, Bhuyan M K, Bose S, Ayyub P, Krishnarmurthy M and Kumar G R 2007 *Appl. Phys.* B **88** 167
[10] Paz V, Emons M and Obata K 2012 *J. Laser Appl.* **24** 042004
[11] Chen A, Kamura M, Kamatra K and Lyoda T 2008 *Adv. Mater.* **20** 763
[12] Goda T and Iyoda T 2012 *J. Mater. Chem.* **22** 9477
[13] Barone P, Barberio M, Stranges F and Xu F 2014 *J. Chem.* **2014** 204028
[14] Barberio M, Barone P, Imbrogno A, Bonanno A and Xu F 2014 *Open J. Compos. Mater.* **4** 78
[15] Barberio M, Stranges F and Xu F 2014 *Appl. Surf. Sci.* **334** 174–9
[16] Amendola V and Meneghetti M 2013 *Phys. Chem. Chem. Phys.* **15** 3027
Fjtik A and Henglein A 1993 *Ber. Bunsen-Ges. Phys. Chem.* **97** 252
Sibbald M S, Chumanova G and Cotton T M 1996 *J. Phys. Chem.* **100** 4672
[17] Kelly K L, Coronado E, Zhao L L and Schatz G C 2003 *J. Phys. Chem.* B **107** 668
[18] Barone P, Barberio M, Oliva A and Bonanno A 2012 *Part. Part. Syst. Charact.* **28** 64
[19] Palik E D 1998 *Handbook of Optical Constant of Solids* (New York: Academic)
[20] Barberio M, Barone P, Xu F and Bonanno A 2013 *J. Chem. Chem. Eng.* **7** 1142–8
[21] NIST XPS database (http://srdata.nist.gov/xps/)